Journal of Sound and Vibration (1998) **211**(4), 537–554

A VIBROACOUSTIC MODEL FOR HIGH FREQUENCY ANALYSIS

A. LE BOT

Laboratoire de Tribologie et Dynamique des Structures, UMR CNRS 5513 *Dynamique des Systèmes et des Structures, Ecole Centrale de Lyon*, 36, *avenue Guy de Collongue*, *BP* 163, 69131 *Ecully Cedex, France*

(*Received* 15 *April* 1996, *and in final form* 14 *February* 1997)

A simplified model is presented for medium and high frequencies in structures or acoustics. This model, which does not take into account interferences between propagative waves, is asymptotic in the sense that it is more accurate as frequency increases. Based on energetic quantities and energy balance, the spirit of *Statistical Energy Analysis* (SEA) is conserved. But, unlike SEA which involves global variables, this model considers local variables. The description is more precise and, in particular, the repartition of energy density inside each sub-system is predicted. Numerical simulations are presented, which indicate that the results of this model are a good frequency average of the exact response and are close to those of the ray tracing technique.

1. INTRODUCTION

Medium and high frequencies have received less attention from researchers than low frequencies. However, the success of modern techniques such as *Statistical Energy Analysis* (SEA) for vibroacoustic and the ray tracing for room acoustics indicate the interest in engineering to use such methods. Both methods have been applied with considerable success and have proved their efficiency for industrial appplications. More recently, there has been interest in generalizing these methods and correcting some of their shortcomings. For instance, the predictive determination of coupling loss factors in SEA with an acceptable accuracy is a major problem. So, many users prefer to use SEA as a semi-empirical model by measuring the coupling loss factors. On the other hand, ray tracing is an efficient method widely employed to solve problems in room acoustics especially when the Sabine formula is not valid. But the equivalent technique for structural problem has not yet been significantly developed and the particular problem of vibroacoustics in respect to the ray technique remains an open problem.

For a number of years, various approaches have been attempted to generalize the SEA beyond its limits of application. One of these, called *Energy Flow Analysis or Power Flow Finite Element Analysis* [1], uses the same quantities as in SEA; energy and energy flow, and is based on an equation similar to the heat conduction equation in steady state. This differential equation leads to a continuous analysis of structures whereas SEA is based on a discrete analysis. The particular case of one-dimensional systems such as rod or beam have been well studied [1–3]. But the multi-dimensional case was first investigated by way of a direct generalization of the thermal analogy established for the one-dimensional space [1]. This generalization has proven to be valid for travelling plane waves in reference [4] and for a diffuse field in references [5, 6]. This generalization was criticized by Langley [6, 7]

0022–460X/98/140537 + 18 $25.00/0/sv971378

who remarked that, for an infinite structure, the decrease in the far-field of the heat conduction equation solution is in contradiction with those of the energy density deduced from the Helmholtz equation. In agreement with Langley [6], LeBot *et al*. [8] suggested an explanation of this paradox which points out a limitation of the thermal analogy. But this explanation uses the particular symmetry of infinite systems and does not propose a solution for general geometry without symmetry.

The aim of the present paper is to propose an alternative method to the heat conduction equation for multi-dimensional systems such as plates or acoustical enclosures.

In section 2.1, the direct field is investigated by studying infinite systems. It is shown that, unlike the heat conduction equation, the analytical solution obtained here is in agreement with the exact result deduced from classical equations of motion. Next, the diffracted field is taken into account by applying Huygens principle [9]. Then an integral represention of energy fields is obtained in section 2.2. The fictive sources distributed among the boundary are evaluated in section 2.3. At each point of the boundary, an energy balance is stated and then fictive sources are found to satisfy an integral Fredholm equation of the second kind. In section 2.4, the same method is applied to the structural coupling problem. This leads to two integral Fredholm equations. These equations are solved in section 3 by using the classical collocation method. Finally, two numerical illustrations are presented: the first concerns a couple of square plates and the second an acoustical enclosure.

2. THEORITICAL FORMULATION

Two energy quantities are involved in this formulation: the energy density W is defined as the sum of the kinetic and the potential energies (or deformation energy for structures) and the energy flow vector $\mathbf{I}$ which supports the motion of energy inside systems. Moreover the group velocity c_g is needed as a characteristic of the system. A first set of assumptions required to derive the energy model is summarized as follows: (H1) linear, isotropic, homogeneous system in steady state conditions excited in a broadband centred on ω; (H2) light damping loss factor; (H3) evanescent waves and near-field are neglected; (H4) interferences between propagative waves are not taken into account. The necessity for assumptions (H1)–(H4) will be highlighted in the course of subsequent developments. Another assumption will be added later on.

The first step to establish this energy formulation is the well known power balance for a local region:

$$\mathbf{div}\,.\,\mathbf{I} + p_{diss} = p_{inj}\,. \tag{1}$$

Here p_{diss} is the power density being dissipated and p_{inj} the injected power density supplied by sources. Observe that no accumulation term occurs in this power balance by virtue of the steady state assumption in (H1). (A list of notation is given in Appendix C.)

The power density being dissipated is proportional to one form of energy. For instance, for a viscous model, the power density being dissipated is proportional to the kinetic energy density. In opposition, hysteretic damping leads to a proportionality to potential energy density. For a pure propagative wave and with the nearfield and evanescent waves neglected, it is laborious but not difficult to verify for several system examples that kinetic and potential energy densities are equal [10]. An example of such a calculation is fully developed in Appendix A. Moreover, with interferences between propagative waves neglected as previously specified in (H4), this equality between the two forms of energy remains valid for a more complete wave field constructed as a superposition of propagative waves. Hence, two models of dissipation are considered below. The first one is the same

as in SEA with $p_{diss} = \eta\omega W$ where η is the hysteretic damping loss factor of structures. The second one is related to an atmospheric absorption for acoustical enclosures $p_{diss} = mc_g W$ where m is the attenuation coefficient and c_g is the acoustical group velocity. Note that, for the sake of simplicity, the standard definition of the attenuation coefficient which is m times $10 \log e$ and is usually given in dB/m, is not used here.

This energetic formulation is established in two steps. First, pure propagative waves are considered. Their role is similar to those of the elementary solution of classical differential problems. Second, more complete wave fields are considered.

2.1. PROPAGATIVE WAVES

Of particular interest are propagative waves in a system. These can be of many kinds. But, for the purpose of constructing complete fields, one is interested only in one sort of travelling waves, which are *fields created by a single point source S and propagating in an infinite system*. These are plane waves for one-dimensional systems, cylindrical waves for two-dimensional systems and spherical waves for three-dimensional systems. So, in all the text, "propagative waves" means these particular propagative waves without specifying any restriction.

As space is isotropic, these waves are symmetric around the source point S. So, their fields depend only on the distance r between the observation point M and the source S. In particular, the intensity $\mathbf{I}$ has just a radial component, the algebraic value of which is denoted by I. One can rewrite the power balance (1) as

$$\frac{1}{r^{n-1}} \frac{\mathrm{d}}{\mathrm{d}r} (r^{n-1} I) + mc_g W = 0, \tag{2}$$

where n is the dimension of the space under consideration ($n = 1$, 2 or 3). m could be replaced by $\eta\omega/c_g$ for hysteretic damping. Propagative waves are characterized by an especially simple relationship between the energy flow and the energy density [10]: a proportionality coefficient which is exactly the group velocity; $I(r) = c_g W(r)$. Thus, the equality is

$$\mathbf{I}(M) = c_g W(M) \mathbf{u}_{SM}, \tag{3}$$

where $\mathbf{u}_{SM}$ is the unit vector from the source S toward the observation point M. This relationship is valid in the far field for outgoing travelling waves (and not for evanescent wave) and for an undamped system. For a lightly damped system (H2), this relationship remains valid upon taking into account the dissipation by way of the dissipative term in the power balance (1). A proof of this assertion is given in Appendix A for plate structures. So, by substituting this constitutive equation (3) into the power balance (2) , a first order differential equation on $W(r)$ alone is obtained:

$$\frac{1}{r^{n-1}} \frac{\mathrm{d}}{\mathrm{d}r} (r^{n-1} W) + mW = 0. \tag{4}$$

Solving this equation gives the energy quantities W and $\mathbf{I}$ of propagative waves which are respectively proportional to the functions

$$G(S, M) = \frac{\mathrm{e}^{-mr}}{r^{n-1}} \quad \text{and} \quad \mathbf{H}(S, M) = c_g \frac{\mathrm{e}^{-mr}}{r^{n-1}} \mathbf{u}_{SM}, \tag{5}$$

where r is the distance between S and M and the factor $\eta\omega/c_g$ could replace m in case of structural damping. These functions will often be invoked below as they play a crucial role when one constructs more complete wave fields. It can be observed that a reciprocity

relationship is satisfied, $G(S, M) = G(M, S)$, as G depends only on the distance r according to the homogeneity and isotropy of space.

These solutions (5) can be compared with a well-known result of the equation of motion. In the case of an infinite membrane, the analytical solution of the equation of transverse motion is the Hankel function of order zero and second kind $H_0^{(2)}(kr)$ where k is the complex wavenumber. A similar argument as used in Appendix A leads to the energy density $W(r) \propto e^{-\eta k_0 r}/r$ where k_0 is the undamped wavenumber. It should be added that membranes are nondispersive systems so $k_0 = \omega/c_g$ and then $W(r) \propto e^{-\eta\omega r/c_g}/r$. This result has to be compared with $G(S, M)$ given in equation (5). Unlike this, the asymptotic development of the solution of the heat conduction equation is [6, 8] $e^{-\eta\omega r/c_g}/\sqrt{r}$. The decrease is like $1/\sqrt{r}$ in opposition with $1/r$ for the exact result. This contradiction points out that the heat conduction equation and the method proposed below are truly not equivalent. Indeed both methods involve the same quantities W and $\mathbf{I}$ and depend on power balance, then they are close each other. But fields stemming from the heat conduction equation are constructed as a superposition of plane waves whilst the fields here are cylindrical waves for two-dimensional structures and spherical waves for acoustic space.

One can now try to find the local power balance satisfied by the field G and $\mathbf{H}$. Obviously, as they have been constructed for this, everywhere except at S itself, the homogeneous version ($p_{inj} = 0$) of the power balance (1) is satisfied by G and $\mathbf{H}$. But the question is, what is the injected power density exactly at S? The full explanation is given in Appendix B. G and $\mathbf{H}$ are identified as distributions and the differential operator occuring in equation (1) is taken in the distribution sense. The result is

$$\mathbf{div}_M \,.\, \mathbf{H}(S, M) + mc_g G(S, M) = \gamma_0 c_g \delta_S(M), \tag{6}$$

where γ_0 is the solid angle of space at hand. This means that the fields G and $\mathbf{H}$ are the elementary solutions of the power balance (1) which satisfy equation (3).

2.2. COMPLETE WAVE FIELDS

In general, many propagative waves travel simultaneously in a given system. The problem now is to establish the fields W and $\mathbf{I}$ for any domain Ω bounded or not and submitted to any excitation. The boundary of the domain Ω is noted $\partial\Omega$. Two principles are invoked: a linear superposition principle and Huygens principle.

First of all, consider the equation of motion $\mathbf{L}\boldsymbol{\psi} = \mathbf{g}$ of a structure. $\mathbf{L}$ is a linear operator, $\boldsymbol{\psi}$ the unknown field (pressure for acoustic or displacement vector for structures) and $\mathbf{g}$ the source term. Indeed the linear superposition principle is valid for such an equation. So, if ψ_1 and ψ_2 are two propagative fields associated with the point source terms δ_{S_1} and δ_{S_2} and subject to the Sommerfeld radiation condition, then $\psi_1 + \psi_2$ is the field associated with the source $\delta_{S_1} + \delta_{S_2}$. The energy density W is now obtained by squaring the fields:

$$W = \beta|\psi_1 + \psi_2|^2 = \beta|\psi_1|^2 + 2\beta R_e\{\psi_1\psi_2^*\} + \beta|\psi_2|^2 = W_1 + 2\beta R_e\{\psi_1\psi_2^*\} + W_2. \tag{7}$$

Here β is a constant depending on the characteristics of the system and W_1 and W_2 are the energy densities of ψ_1 and ψ_2 separately. According to (H4) interferences between propagative waves are neglected. This means that the cross product $2\beta R_e\{\psi_1\psi_2^*\}$ can be removed in expression (7). Thus, the energy density of a superposition of simple fields is merely the sum of the energy densities of each field. This is the linear superposition principle extended to energy quantities.

Linear superposition principle: *Energy quantities of a superposition of simple propagative fields are merely the sums of the energy quantities of each propagative field.*

The removal of the middle term in equation (7) has been interpreted in various ways in the literature. For instance, in reference [2], space averages over a half-wavelength are considered. The average of this interfering term is then found to vanish.

Second, following Huygens principle, the most general field comes from the superposition of a direct field emerging from actual sources located in the domain and a diffracted field emerging from fictive sources located on the boundary of the domain.Usually, Huygens principle is involved for classical kinematic fields. For instance, the Helmholtz–Kirchhoff formula gives an integral representation of any acoustical field governed by the Helmholtz equation. This formula indicates that the diffracted field is constructed as the superposition of a single and a double layer potential. The originality of the present model is that Huygens principle is applied directly to energy quantities. Obviously, in this respect, Huygens principle is adopted here as a premise, and hence does not require prior justification.

Huygens principle: *At any point* M, *the functions* $W(M)$ *and* $\mathbf{I}(M)$ *are the superposition of a direct field created by primary sources* (*or actual sources*) ρ *located at* S *inside* Ω. $\rho(S)G(S, M)$ *and* $\rho(S)\mathbf{H}(S, M)$, *and a diffracted field created by secondary sources* (*or fictive sources*) σ *located at* P *on* $\partial\Omega$, $\sigma(P)f(\mathbf{u}_{MP}, \mathbf{n}_P)G(P, M)$ *and* $\sigma(P)f(\mathbf{u}_{MP}, \mathbf{n}_P)\mathbf{H}(P, M)$.

The secondary sources have a directivity diagram f which depends on the angle between the direction $\mathbf{u}_{MP}$ of the emission and the outward normal vector $\mathbf{n}_P$ at point P. This function is subject to an additional assumption: (H5) all fictive sources have the same directivity diagram f which does not depend on the point P.

All these considerations are summarized the following relationships:

$$W(M) = \int_\Omega \rho(S)G(S, M)\,\mathrm{d}S + \int_{\partial\Omega} \sigma(P)f(\mathbf{u}_{MP}, \mathbf{n}_P)G(P, M)\,\mathrm{d}P, \tag{8}$$

$$\mathbf{I}(M) = \int_\Omega \rho(S)\mathbf{H}(S, M)\,\mathrm{d}S + \int_{\partial\Omega} \sigma(P)f(\mathbf{u}_{MP}, \mathbf{n}_P)\mathbf{H}(P, M)\,\mathrm{d}P. \tag{9}$$

Here ρ and σ are respectively the magnitudes of the primary and the secondary sources. Indeed, the primary sources ρ are assumed to be known because actual sources constitute data of the problem. But the secondary sources σ are unknown and an equation which determines their value has to be exhibited. This is the topic of section 2.3.

The validity domain of the assumption (H4) has not yet been defined. As specified by Huygens principle, propagative waves can emerge from both primary and secondary sources. To neglect interferences of propagative waves created by primary sources is valid under the condition that all excitation points are uncorrelated. On the other hand, to neglect interferences of the diffracted field refers to situations where the modal behavior of the system is irrelevant. This occurs in the high frequency domain especially when the modal overlap is high.

It is interesting to note that equations (8) and (9) can be derived directly from the Helmholtz–Kirchhoff integral representation for the acoustical case. For an interior or exterior problem, the acoustical pressure p at any point M of the domain Ω is

$$p(M) = \int_\Omega a(S)g(S, M)\,\mathrm{d}S + \int_{\partial\Omega} \left[\frac{\partial p}{\partial n}(P)g(P, M) - p(P)\frac{\partial g}{\partial n}(P, M)\right]\mathrm{d}P, \tag{10}$$

where $\partial./\partial n$ means the outward normal derivative and $g(A, B) = \mathrm{e}^{-\mathrm{i}kr}/4\pi r$ with $r = |AB|$ is the Green function for the infinite system. The wavenumber k can be a complex number

to take into account the atmospheric absorption $k = k_0 - \mathrm{i}m/2$. The total energy density W is deduced from the pressure as

$$W(M) = \frac{1}{4\rho c^2}|p|^2(M) + \frac{1}{4\rho\omega^2}\,|\mathbf{grad}\,p|^2(M), \tag{11}$$

where ρ is the density of the fluid and c the sound speed. One can now substitute equation (10) in the relationship (11). The squared integrals or cross product appearing can be rewritten as integrals over the Cartesian products $\Omega \times \Omega$, $\Omega \times \partial\Omega$ and $\partial\Omega \times \partial\Omega$. Now, the assumption (H4) is interpreted in this way: in the integrand of an integral over $A \times B$, only the terms due to the same point (P, P) are retained, the other terms are due to interferences; then,

$$\left\langle \int_{A\times B} f(P)g(Q)\,\mathrm{d}P\,\mathrm{d}Q \right\rangle = \mu \int_{diag\,A\times B} f(P)g(P)\,\mathrm{d}P, \tag{12}$$

where $\langle\,.\,\rangle$ means that interferences have been removed and μ is necessary for dimensionality. The operator $\langle\,.\,\rangle$ may be viewed as an ensemble average in the following way. Upon assuming that the functions f and g are statistically independent, an ensemble average would yield $\langle f(P)g(Q)\rangle = \mu f(P)g(P)\delta_P(Q)$. Then equation (12) is a consequence of this relationship. After evaluating these terms, one has

$$\begin{aligned}\langle W\rangle(M) = {} & \mu_\Omega \int_\Omega |a|^2(S)\left\{\frac{1}{4\rho c^2}\,|g|^2 + \frac{1}{4\rho\omega^2}\,|\mathbf{grad}_M g|^2\right\}\mathrm{d}S \\ & + \mu_{\partial\Omega}\int_{\partial\Omega}\left|\frac{\partial p}{\partial n}\right|^2(P)\left\{\frac{1}{4\rho c^2}\,|g|^2 + \frac{1}{4\rho\omega^2}\,|\mathbf{grad}_M g|^2\right\}\mathrm{d}P \\ & - 2\mu_{\partial\Omega}R_e\int_{\partial\Omega}\frac{\partial p}{\partial n}\,p^*(P)\left\{\frac{1}{4\rho c^2}\,g\,\frac{\partial g^*}{\partial n} + \frac{1}{4\rho\omega^2}\,\mathbf{grad}_M g\,.\,\mathbf{grad}_M\frac{\partial g^*}{\partial n}\right\}\mathrm{d}P \\ & + \mu_{\partial\Omega}\int_{\partial\Omega}|p|^2(P)\left\{\frac{1}{4\rho c^2}\left|\frac{\partial g}{\partial n}\right|^2 + \frac{1}{4\rho\omega^2}\left|\mathbf{grad}_M\frac{\partial g}{\partial n}\right|^2\right\}\mathrm{d}P.\end{aligned} \tag{13}$$

Six functions derived from g appear in this relationship. All of them can be analytically evaluated from the explicit expression for g. But using the far field assumption (H3) and the light damping assumption (H2), some drastic simplifications are realized and finally all these functions are found to be proportional to the previous function G: for instance,

$$|g|^2 = \frac{\mathrm{e}^{-mr}}{16\pi^2 r^2} = \frac{1}{16\pi^2}\,G, \qquad |\mathbf{grad}_M g|^2 = \frac{\mathrm{e}^{-mr}}{16\pi^2 r^2}\left|\mathrm{i}k + \frac{1}{r}\right|^2 \approx \frac{|k_0|^2}{16\pi^2}\,G, \ldots . \tag{14}$$

This last equality stems from a first order development for small m/k_0 (H2) and a second order development for small $1/k_0 r$ (H3). Then

$$\langle W\rangle(M) = \int_\Omega \frac{\mu_\Omega}{32\pi^2\rho c^2}\,|a|^2(S)G(S, M)\,\mathrm{d}S$$

$$+ \int_{\partial\Omega} \frac{\mu_{\partial\Omega}}{32\pi^2\rho c^2}\left\{\left|\frac{\partial p}{\partial n}\right|^2 - 2R_e\left(\mathrm{i}k^*\frac{\partial p}{\partial n}p^*\right)\mathbf{u}_{PM}\,.\,\mathbf{n}_P\right.$$

$$\left. + |kp|^2(\mathbf{u}_{PM}\,.\,\mathbf{n}_P)^2\right\}G(P, M)\,\mathrm{d}P, \tag{15}$$

where G is the function given by (5) and $\mathbf{u}_{PM}$ is the unit vector from P to M. This is exactly the same form as expression (8). An equivalent relationship is obtained for $\langle\mathbf{I}\rangle(M)$.

2.3. BOUNDARY CONDITION

This expected equation for σ is obtained by applying the power balance on the boundary $\partial\Omega$. At any point P on the boundary, the incident power comes from both the direct field and the diffracted field. The boundary is characterized by an absorption coefficient α lying between 0 and 1 which is defined as the ratio of absorbed power to incident power. This coefficient α may depend on the point P. The reflected power emitted by the secondary source $\sigma(P)$ at point P is equal to the incident power minus the absorbed power. It can be written as

$$P_{emit} = (1 - \alpha_P)\{P_{dir} + P_{dif}\}, \tag{16}$$

where each term is the infinitesimal power emitted or received from a solid angle $\mathrm{d}\theta$ by an infinitesimal surface $\mathrm{d}P$ surrounding P. Notations are defined in Figure 1.

First, consider the emitted power. It is the flux of the intensity created by the source of magnitude $\sigma(P)\,\mathrm{d}P$ through a part of the sphere of radius ε (surface $\varepsilon^{n-1}\,\mathrm{d}\theta$) corresponding to the emitted direction:

$$P_{emit} = c_g\sigma(P)\,\mathrm{d}Pf(\mathbf{u}_{P'P}, \mathbf{n}_P)\lim_{\epsilon\to 0}\left(\frac{\mathrm{e}^{-m\epsilon}}{\epsilon^{n-1}}\epsilon^{n-1}\,\mathrm{d}\theta\right) = c_g\sigma(P)\,\mathrm{d}Pf(\mathbf{u}_{P'P}, \mathbf{n}_P)\,\mathrm{d}\theta. \tag{17}$$

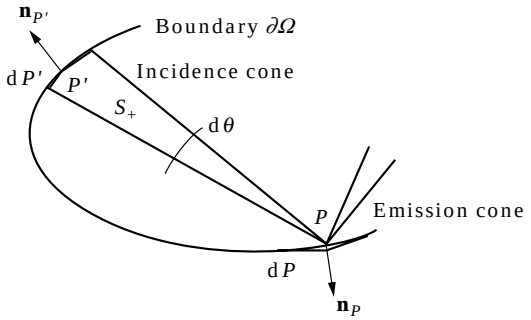

Figure 1. Power balance on the boundary at point P. The power emitted by a fictive source located inside $\mathrm{d}P$ is toward the emission cone and the incident power comes from both actual sources located at S and the fictive source located at P'.

TABLE 1

Values of the coefficient γ, n is the dimension of space at hand and f is the directivity of fictive sources; $f = 1$ is a constant directivity; $f = \mathbf{u} \,.\, \mathbf{n}$ the directivity equals the cosine of the angle between emission direction $\mathbf{u}$ *and the normal to the boundary* $\mathbf{n}$ *(Lambert's law); $f = (\mathbf{u} \,.\, \mathbf{n})^2$ the directivity equals the square of the cosine of previous angle*

	$n = 1$	$n = 2$	$n = 3$
$f = 1$	$\gamma = 2$	$\gamma = \pi$	$\gamma = 2\pi$
$f = \mathbf{u} \,.\, \mathbf{n}$	$\gamma = 2$	$\gamma = 2$	$\gamma = \pi$
$f = (\mathbf{u} \,.\, \mathbf{n})^2$	$\gamma = 2$	$\gamma = \pi/2$	$\gamma = 2\pi$

Second, the incident power of the direct field is the flux through the surface $\mathrm{d}P$ of energy flow from actual sources of magnitude $\rho(S)$ located in the cone of the vertex P and solid angle $\mathrm{d}\theta$:

$$P_{dir} = \int_{P'P} \rho(S)\mathbf{H}(S, P)SP^{n-1}\,\mathrm{d}\theta\,\mathrm{d}S \,.\, \mathbf{n}_P\,\mathrm{d}P. \tag{18}$$

Here $SP^{n-1}\,\mathrm{d}\theta\,\mathrm{d}S$ is the infinitesimal volume in general spherical co-ordinates, and the integral is performed over a segment $P'P$. The scalar product $\cdot\mathbf{n}_P\,\mathrm{d}P$ stems from the calculation of the flux.

Finally, the incident power from the diffracted field is the flux over the surface $\mathrm{d}P$ of energy flow from the fictive source P' of magnitude $\sigma(P')\,\mathrm{d}P$:

$$P_{dif} = \sigma(P')\,\mathrm{d}P' f(\mathbf{u}_{PP'}, \mathbf{n}_{P'})\mathbf{H}(P', P) \,.\, \mathbf{n}_P\,\mathrm{d}P. \tag{19}$$

Note that $\mathrm{d}P'$ is the part of the boundary covered by the solid angle $\mathrm{d}\theta$. After equating and integrating the result over the half-sphere HS_P of inward directions at P with respect to $\mathrm{d}\theta$, one obtains

$$\int_{\mathrm{HS}_P} c_g\sigma(P)f(\mathbf{u}_\theta, \mathbf{n}_P)\,\mathrm{d}\theta = (1 - \alpha_P)\left[\int_{\mathrm{HS}_P}\int_{P'P} \rho(S)\mathbf{H}(S, P)SP^{n-1}\,\mathrm{d}S\,\mathrm{d}\theta \right.$$

$$\left. + \int_{\partial\Omega} \sigma(P')f(\mathbf{u}_{PP'}, \mathbf{n}_{P'})\mathbf{H}(P', P)\,\mathrm{d}P'\right] \,.\, \mathbf{n}_P, \tag{20}$$

where $\mathbf{u}_\theta$ is the unit vector for the direction θ. The second sum is established by remarking that when the direction θ covers the half-sphere HS_P, the point P' entirely covers the boundary $\partial\Omega$. The first sum can be transformed by integration over Ω:

$$\sigma(P) = \frac{1 - \alpha_P}{\gamma c_g}\left\{\int_\Omega \rho(S)\mathbf{H}(S, P)\,\mathrm{d}S + \int_{\partial\Omega} \sigma(P')f(\mathbf{u}_{PP'}, \mathbf{n}_{P'})\mathbf{H}(P', P)\,\mathrm{d}P'\right\} \,.\, \mathbf{n}_P. \tag{21}$$

Here

$$\gamma = \int_{HS} f(\mathbf{u}_\theta, \mathbf{n})\, d\theta \tag{22}$$

has a value depending on the dimension n of the space. Table 1 summarizes these values.

Evidently, equation (21) is a Fredholm integral equation of the second kind on the layer σ.

2.4. COUPLING CONDITIONS

Now consider two systems Ω_1 and Ω_2 coupled along a common boundary $\partial\Omega_1 \cap \partial\Omega_2$. Indeed, Huygens principle remains valid and inside each system i the fields W_i and $\mathbf{I}_i$ are obtained with the relationships (8) and (9) where Ω and $\partial\Omega$ are respectively replaced by Ω_i and $\partial\Omega_i$. Moreover, at each point P of the boundary which is not located on the interface $\partial\Omega_1 \cap \partial\Omega_2$, the boundary condition (21) still applies. But, at a point P on the common boundary $\partial\Omega_1 \cap \partial\Omega_2$, two fictive potentials σ_i are now involved, one on each side of the boundary. So, two coupling conditions on these potentials are expected at this point P.

These coupling conditions are derived in the same way as the previous boundary condition (21): i.e., by applying the power balance on the interface $\partial\Omega_1 \cap \partial\Omega_2$. This power balance was proposed by Cho and Bernhard [11, 12] for an interface between beams. It can be summarized as follows. At a point P on the common boundary $\partial\Omega_1 \cap \partial\Omega_2$, the emitted energy toward Ω_1 is the sum of the reflected energy coming from Ω_1 and the transmitted energy coming from Ω_2. In the same way, the energy emitted toward Ω_2 is the sum of the transmitted energy coming from Ω_1 and the reflected energy coming from Ω_2. So, upon introducing a reflection efficiency r and a transmission efficiency t which are defined respectively as the ratio of the reflected power to the incident power and the transmitted power to the incident power, the infinitesimal power balances take the forms

$$P_{1,emit} = r\{P_{1,dir} + P_{1,dif}\} + t\{P_{2,dif} + P_{2,dif}\}, \tag{23}$$

$$P_{2,emit} = t\{P_{1,dir} + P_{1,dif}\} + r\{P_{2,dir} + P_{2,dif}\}, \tag{24}$$

where the subscripts designate the domain into consideration. The ratios r and t depend on the angles of incidence θ_1 and refraction θ_2. The angles θ_i are related by the Snell–Descartes law of refraction

$$(1/c_{\varphi_1}) \sin\theta_1 = (1/c_{\varphi_2}) \sin\theta_2, \tag{25}$$

where c_{φ_i} is the phase velocity of the domain Ω_i. Figure 2 clarifies the notations.

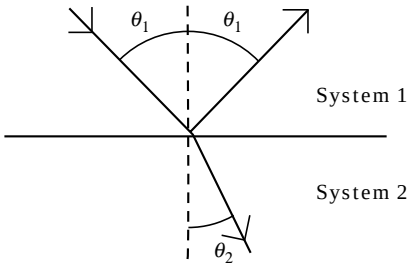

Figure 2. Incident angle θ_1 and refracted angle θ_2.

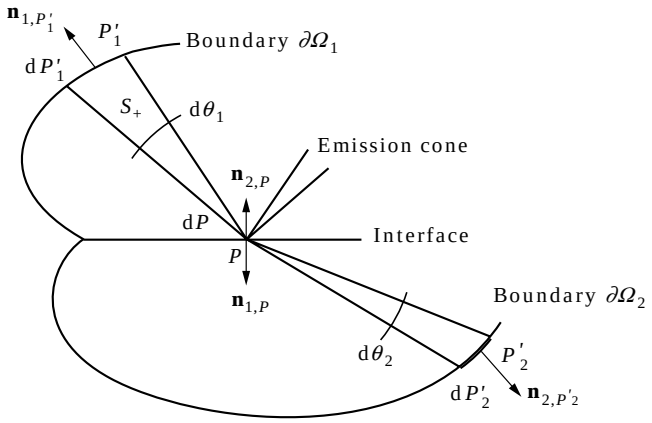

Figure 3. Power balance on the interface at point P. Two fictive sources are located on each face of the infinitesimal surface $\mathrm{d}P$ and the incident powers come from both actual sources located at S and fictive sources located at P'_1 and P'_2.

A classical determination for plane waves in optics or acoustics leads to the relationships

$$r = \left(\frac{Z_2 \cos\theta_1 - Z_1 \cos\theta_2}{Z_2 \cos\theta_1 + Z_1 \cos\theta_2}\right)^2, \qquad t = \frac{4Z_1 Z_2 \cos\theta_1 \cos\theta_2}{(Z_2 \cos\theta_1 + Z_1 \cos\theta_2)^2}, \tag{26, 27}$$

where Z_i is the impedance of the system. For membranes one has $Z_i = \rho_i c_{\varphi_i}$ where ρ_i is the surface mass density. For acoustics the same relationship applies with ρ_i the volumetric mass density. But for plates, evanescent waves modify the behavior in the vicinity of the common boundary. By taking into account the continuity of displacement, slope, bending moment and transverse force, some expressions different from equations (26, 27) can be established. These are fully determined in reference [13].

One can now evaluate all the terms occuring in the power balances (23, 24). With reference to Figure 3 for notations, the emitted powers are

$$P_{i,emit} = c_{g_i}\sigma_i(P) f(\mathbf{u}_{P'_i P}, \mathbf{n}_{i,P})\, \mathrm{d}\theta_i\, \mathrm{d}P, \tag{28}$$

and the incident powers of the direct fields are

$$P_{i,dir} = \int_{P'_i P} \rho(S)\mathbf{H}_i(S, P) \,.\, \mathbf{n}_{i,P} SP^{n-1}\, \mathrm{d}S\, \mathrm{d}\theta_i\, \mathrm{d}P. \tag{29}$$

Finally, the incident powers from the diffracted fields are

$$P_{i,diff} = \sigma_i(P'_i) f(\mathbf{u}_{PP'_i}, \mathbf{n}_{i,P'_i}) \mathbf{H}_i(P'_i, P) \cdot \mathbf{n}_{i,P}\, \mathrm{d}P'_i\, \mathrm{d}P. \tag{30}$$

After integrating over all the incident angles, the following two coupling conditions are obtained:

$$\sigma_1(P) = \frac{1}{\gamma c_{g_1}} \left\{ \int_{\Omega_1} r\rho(S)\mathbf{H}_1(S, P)\, \mathrm{d}S + \int_{\partial\Omega_1} r\sigma_1(P') f(\mathbf{u}_{PP'}, \mathbf{n}_{1,P'}) \mathbf{H}_1(P', P)\, \mathrm{d}P' \right\} \cdot \mathbf{n}_{1,P}$$

$$+ \left\{ \int_{\Omega_2} t\rho(S)\mathbf{H}_2(S, P)\, \mathrm{d}S + \int_{\partial\Omega_2} t\sigma_2(P') f(\mathbf{u}_{PP'}, \mathbf{n}_{2,P'}) \mathbf{H}_2(P', P)\, \mathrm{d}P' \right\} \cdot \mathbf{n}_{2,P}, \tag{31}$$

$$\sigma_2(P) = \frac{1}{\gamma c_{g_2}} \left\{ \int_{\Omega_1} t\rho(S)\mathbf{H}_1(S, P)\, \mathrm{d}S + \int_{\partial\Omega_1} t\sigma_1(P')\, f(\mathbf{u}_{PP'}, \mathbf{n}_{1P'})\mathbf{H}_1(P', P)\, \mathrm{d}P' \right\} \cdot \mathbf{n}_{1,P}$$

$$+ \left\{ \int_{\Omega_2} r\rho(S)\mathbf{H}_2(S, P)\, \mathrm{d}S + \int_{\partial\Omega_2} r\sigma_2(P')\, f(\mathbf{u}_{PP'}, \mathbf{n}_{2,P'})\mathbf{H}_2(P', P)\, \mathrm{d}P' \right\} \cdot \mathbf{n}_{2,P}. \tag{32}$$

Equations (8), (9), (21), (31) and (32) are the basic relationships of the present model. The features of such a formulation are really interesting. In what follows, a numerical implementation is first developed and then two examples are considered.

3. NUMERICAL IMPLEMENTATION

The collocation procedure employed for solving the above system of Fredholm equations is now developed. To solve the system of equations (8), (9), (21), (31) and (32), the boundary $\partial\Omega$ is divided into flat segments Σ_i, $i = 1, n$ (see Figure 4) and the discrete curve is assumed to be an accurate estimation of the actual boundary.

P_i denotes the middle of the segment Σ_i, $\mathbf{n}_i$ the outward normal vector at point P_i and α_i the absorption coefficient at P_i. It is assumed that the layer σ is constant over Σ_i, the value of which is noted σ_i. This is the simplest choice of discontinuous interpolation. However, these discontinuous boundary elements have been commonly used in codes based on the classical integral representation formula of Helmholtz and have demonstrated their efficiency.

Therefore the Fredholm equation (21) with p point sources of magnitude A_k located at S_k becomes

$$\sigma_i = \frac{1}{\gamma c_g} \left\{ \sum_{k=1}^{p} A_k \mathbf{H}(S_k, P_i).\mathbf{n}_i + \sum_{\substack{j=1 \\ j \neq i}}^{n} \sigma_j \int_{\Sigma_j} f(\mathbf{u}_{P_iQ}, \mathbf{n}_j)\mathbf{H}(Q, P_i).\mathbf{n}_i\, \mathrm{d}Q \right\} \quad \text{for } i = 1, n. \tag{33}$$

In the same way, upon assuming that p_l is the number of point sources $S_{l,k}$ located inside Ω_l, the discrete versions of the coupling conditions (31) and (32) are

$$\sigma_{1,i} = \frac{1}{\gamma c_{g_1}} \left\{ \sum_{k=1}^{p_1} A_{1,k} r_i \mathbf{H}_1(S_{1,k}, P_i).\mathbf{n}_{1,i} + \sum_{\substack{j=1 \\ j \neq i}}^{n_1} \sigma_{1,j} \int_{\Sigma_{1,j}} r_i f(\mathbf{u}_{P_iQ}, \mathbf{n}_{1,j})\mathbf{H}_1(Q, P_i).\mathbf{n}_{1,i}\, \mathrm{d}Q \right.$$

$$\left. \sum_{k=1}^{p_2} A_{2,k} t_i \mathbf{H}_2(S_{2,k}, P_i).\mathbf{n}_{2,i} + \sum_{\substack{j=1 \\ j \neq i}}^{n_2} \sigma_{2,j} \int_{\Sigma_{2,j}} t_i f(\mathbf{u}_{P_iQ}, \mathbf{n}_{2,j})\mathbf{H}_2(Q, P_i).\mathbf{n}_{2,i}\, \mathrm{d}Q \right\}, \tag{34}$$

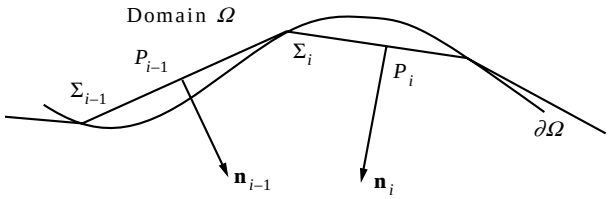

Figure 4. Discrete boundary. The boundary $\partial\Omega$ is divided into flat segments Σ_i with centers at P_i.

$$\sigma_{2,i} = \frac{1}{\gamma c_{g_2}} \left\{ \sum_{k=1}^{p_1} A_{1,k} t_i \mathbf{H}_1(S_{1,k}, P_i) \,.\, \mathbf{n}_{1,i} + \sum_{\substack{j=1 \\ j \neq i}}^{n_1} \sigma_{1,j} \int_{\Sigma_{1,j}} t_i f(\mathbf{u}_{P_i Q}, \mathbf{n}_{1,j}) \mathbf{H}_1(Q, P_i).\mathbf{n}_{1,i} \, \mathrm{d}Q \right.$$

$$\left. \sum_{k=1}^{p_2} A_{2,k} r_i \mathbf{H}_2(S_{2,k}, P_i).\mathbf{n}_{2,i} + \sum_{\substack{j=1 \\ j \neq i}}^{n_2} \sigma_{2,j} \int_{\Sigma_{2,j}} r_i f(\mathbf{u}_{P_i Q}, \mathbf{n}_{2,j}) \mathbf{H}_2(Q, P_i).\mathbf{n}_{2,i} \, \mathrm{d}Q \right\}. \tag{35}$$

The $n_1 + n_2$ unknowns $\sigma_{l,i}$ are determined by solving these equations. Then, the fields W and $\mathbf{I}$ are calculated from

$$W_l(M) = \sum_{k=1}^{p_l} A_{l,k} G_l(S_{l,k}, M) + \sum_{j=1}^{n_l} \sigma_{l,j} \int_{\Sigma_{l,j}} f(\mathbf{u}_{MQ}, \mathbf{n}_Q) G_l(Q, M) \, \mathrm{d}Q, \tag{36}$$

$$\mathbf{I}_l(M) = \sum_{k=1}^{p_l} A_{l,k} \mathbf{H}_l(S_{l,k}, M) + \sum_{j=1}^{n_l} \sigma_{l,j} \int_{\Sigma_{l,j}} f(\mathbf{u}_{MQ}, \mathbf{n}_Q) \mathbf{H}_l(Q, M) \, \mathrm{d}Q. \tag{37}$$

These equations can be solved with an appropriate software.

4. NUMERICAL SIMULATION

The first example is concerned with an acoustical enclosure. The room under study is $30 \times 30 \times 5$ m in size and the absorption coefficient of the walls is 0·5. A point source is located at $10 \times 10 \times 0{\cdot}8$ m and has a power of 1 W. The atmospheric absorption is equal to 0·00261 m^{-1} which is a classical value at 1000 Hz. Two calculations have been performed. The first is realized with a ray tracing software called RAYON2.0 and developed at the EDF company. The second is based on the above formulation (equations 33, 36 and 37). Figures 5(a) and 5(b) show the acoustical pressure in dB inside the reception plane which is 1·5 m above the floor.

One can observe two regions of propagation. The first is the direct field with a high level from 95 to 113 dB. The critical distance for such a room is 7 m. So, the region of the direct field is a sphere with 7 m radius and the source point as centre. It is not surprising that direct fields are the same for both calculations. In fact, equation (5) gives e^{-mr}/r^2 for the direct field of the model: this is exactly the same analytic expression which is implemented in the ray tracing software. What is more surprising is that the agreement between both calculations remains in the region of the reverberant field. In this region, the effect of the second integrals in equations (8) and (9) dominates the direct field. The irregularities in the ray tracing results are due to the lack of rays in certain regions. However, the results of both methods are similar and the plot (Figure 5(c)) along the line represented on the pressure maps reveals that there is no more than a few dBs of difference.

The second example is concerned with a couple of square plates. A hysteretic damping factor is introduced, the value of which is 5% for both plates, but there is no dissipation at the boundaries (absorption coefficient $\alpha = 0$). The left and right boundaries are clamped, the common edge is free and other edges are simply supported (see Figure 6).

The characteristics of the plates are as follows: size 2×2 m, Poisson's ratio $\nu = 0{\cdot}3$, thickness $h = 1$ mm, mass density $\rho = 7800\ \mathrm{kg/m^3}$, all for both plates. The Young's modulus is $2{\cdot}1 \times 10^{11}\ \mathrm{N/m^2}$ for plate 1 and $2{\cdot}1 \times 10^{7}\ \mathrm{N/m^2}$ for plate 2. Two local frames are defined as shown in Figure 6. The driving point is located at $x = 0{\cdot}3$ m and $y = 0{\cdot}3$ m on plate 1 and has a magnitude 1 N constant over the frequency band 10 Hz–10 kHz. The reception points are located at $x = 1$ m and $y = 1$ m on each plate.

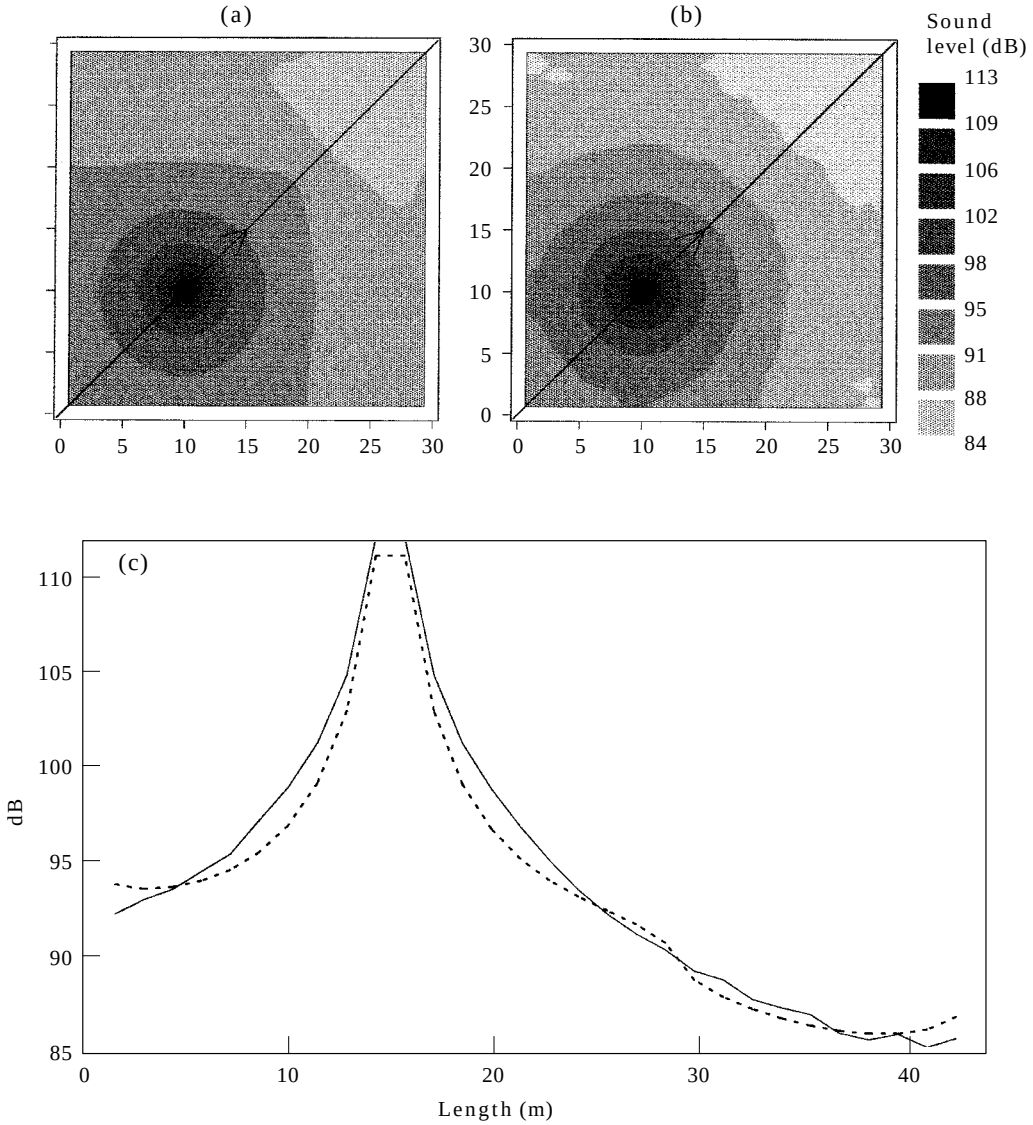

Figure 5. Sound pressure map in a parallelepiped room excited by a point source at $f = 1000$ Hz calculated by two numerical methods. (a) Results obtained by solving the integral equation (21); (b) results obtained by using the ray tracing software RAYON2.0; (c) comparison of both methods along the representative line with an arrow; ------, ray tracing method; —— , integral equation.

A reference calculation is based on a semi-modal development of the solution of the Love plate equation. Energy density and energy flow are then evaluated from the obtained deflection. On the other hand, the above formulation (equations (33)–(37)) is implemented for the second calculation with $\mathbf{u} \cdot \mathbf{n}$ as the directivity diagram. The power of the source is calculated with $P_{inj} = F^2/16\sqrt{D\rho h}$ where D is the rigidity of plate 1. This relationship is the power injected by a force F inside an infinite plate. The magnitude A occurring in equations (31)–(35) obeys $A = P_{inj}/2\pi c_{g_1}$. Results of both calculations are compared in the two parts of Figure 7.

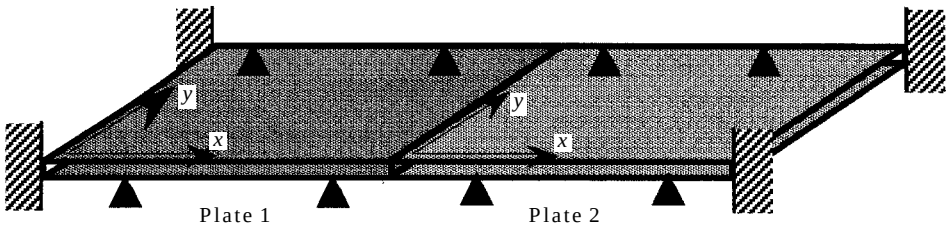

Figure 6. A pair of plates with two different flexural rigidities; plate 1 is excited at a driving point. Left and right edges are clamped, the common boundary is free and other edges are simply supported.

The level of energy is very different from plate 1 to plate 2. This is due to the ratio of group velocities which equals 10. Also, the behavior of this pair of plates differs highly from the behavior of a single plate: features of the coupling edge are not trivial. critical angle at the edge has a small value. Hence, most of the energy propagates from plate 1 to plate 2 but the inverse process is rare. Plate 2 dissipates almost all the energy received from plate 1.

The response calculated with the model is the frequency average of the reference response obtained with a semi-modal decomposition. Indeed, in the energetic model, the modal behavior of the structure is not taken into account because inteferences are neglected. Hence, fluctuations of the reference calculation, due to eigenfrequencies, cannot appear with the model.

5. CONCLUSIONS

This paper has presented an energy formulation for vibrations in structures or acoustical enclosures. By neglecting interferences between propagative waves and using several other minor assumptions, this energy formulation is well suited for the medium and high frequency domains where the modal overlap is high. A smooth response is predicted which can be interpreted as the frequency average of the classical response. Thus, calculations have to be performed in a broad-band $[\omega - \Delta\omega/2, \omega + \Delta\omega/2]$ which contains at least several eigenfrequencies. Moreover, due to the smooth behavior of such responses, few

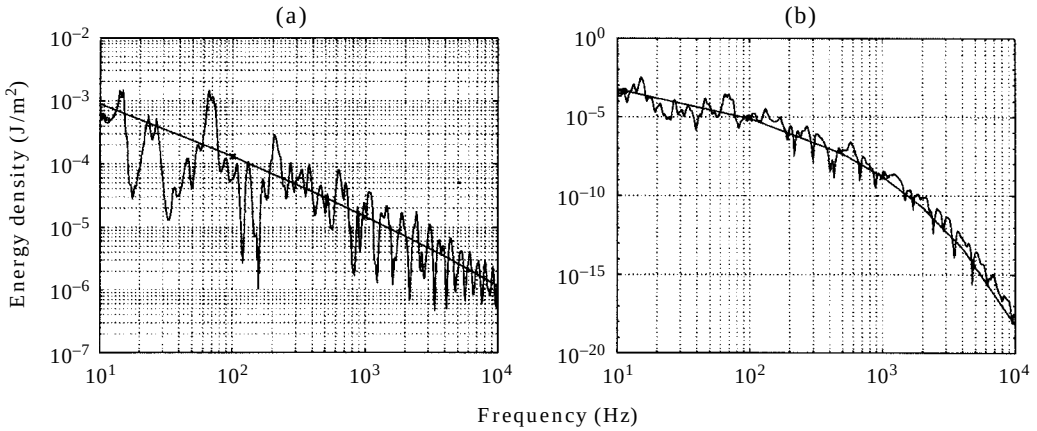

Figure 7. Comparison between two results: smooth curve, integral equation (21); oscillating curve, reference calculation based on a semi-modal development of the solution of the equation of motion. Energy densities; (a) at point 1 on plate 1; (b) at point 2 on plate 2.

degrees of freedom are necessary to solve equations (21), (31) and (32). Hence, this method allows calculations up to high frequencies where the classical methods are usually inefficient. The numerical results obtained indicate that this method is closely similar to the ray tracing technique in acoustics.

ACKNOWLEDGMENTS

The author gratefully acknowledges Mr L. Ricol (DER-EDF département AMV, Clamart, France) for his kind help and advice.

REFERENCES

1. D. J. Nefske and S. H. Sung 1987 *ASME publication NCA* **3**, 47–54. Power flow finite element analysis of dynamic systems: basic theory and application to beams.
2. J. C. Wohlever and R. J. Bernhard 1992 *Journal of Sound and Vibration* **153**, 1–19. Mechanical energy flow models of rods and beams.
3. M. N. Ichchou, A. Le bot and L. Jezequel 1997 *Journal of Sound and Vibration* **201** 535–554 Energy models of one-dimensional, multi-propagative systems.
4. O. Bouthier and R. J. Bernhard 1995 *Journal of Sound and Vibration* **182**, 149–164. Simple models of the energetics of tranversely vibrating plates.
5. M. Djimadoum and J. L. Guyader 1995 *Proceedings of Inter-Noise* 95, *Newport-Beach*, 1217–1220. Possibilities to generalize the heat transfer approach to vibration of plates problems.
6. R. S. Langley 1995 *Journal of Sound and Vibration* **182**, 637–657. On the vibrational conductivity approach to high frequency dynamics for two-dimensional structural components.
7. R. S. Langley 1991 *Journal of Sound and Vibration* **150**, 47–65. Analysis of beam and plate vibrations by using the wave equation.
8. A. Le bot, M. N. Ichchou and L. Jezequel 1995 *Proceedings of Euro-Noise* 95, *Lyon*, 423–428. Smooth energy formulation for multi-dimensional problem.
9. C. Huygens 1690, *Traité de la lumière*. Leyde Neederland, recent edition 1992 Dunod.
10. L. Cremer, M. Heckl and E. E. Ungar 1988, *Structure Borne Sound*. Berlin: Springer-Verlag.
11. P. E. Cho and R. J. Bernhard 1992 *Proceedings of Inter-Noise* 92, *Toronto*, 487–492. Coupling of continuous beam models.
12. P. E. Cho and R. J. Bernhard 1992 *Proceedings of CETIM*, *Senlis France*, 347–354. A simple method for predicting energy flow distributions in frame structures.
13. W. Wöhle, T. Beckmann and H. Schreckenbach 1981 *Journal of Sound and Vibration* **77**, 323–334. Coupling loss factors for Statistical Energy Analysis of sound transmission at rectangular structural slab joints, Part I.
14. H. S. Kim, H. J. Kang and J. S. Kim 1994 *Journal of Sound and Vibration* **174**, 493–504. A vibration analysis of plates at high frequencies by the power flow method.

APPENDIX A: VERIFICATION OF EQUALITY (3)

The following discussion is developed in various manners in references [4, 10, 14]. So, this Appendix collects scattered arguments and just retains the main steps of the calculation, with reference to previous papers for more details in order to highlight how assumptions (H1)–(H3) are necessary for developments occurring in section 2.1.

Here, one is interested in verifying two points. First, for a time-harmonic travelling cylindrical wave in a plate, the kinetic energy density is equal to the potential energy density. Second, for such a wave, energy flow is equal to the energy density times the group velocity.

Consider an infinite thin plate loaded by a transverse time-harmonic point force. The deflection w is a sum of two Hankel functions of the second kind of order zero

$$w = \alpha\{H_0^{(2)}(kr) - H_0^{(2)}(-\mathrm{i}kr)\}, \tag{A1}$$

where $k = k_0(1 - i\eta/4)$ is the complex wavenumber and r is the distance between the source point and the point at hand. The first term is an oscillating function whereas the second term rapidly decreases in the farfield. This evanescent wave can be neglected by virtue of the first part of assumption (H3). Moreover the second part of (H3) states that a large argument $|kr| \gg 1$ development can be retained. It yields

$$w = \alpha \, e^{-i(kr - \pi/4)}/\sqrt{2\pi kr}. \tag{A2}$$

with account taken of the axisymmetry of the problem, the kinetic energy density, potential energy density and energy flow are respectively related to the deflection by

$$T = \frac{1}{4}\rho\omega^2|w|^2, \qquad V = \frac{1}{4}D\left\{\left|\frac{d^2w}{dr^2}\right|^2 + \frac{2v}{r}R_e\left(\frac{d^2w}{dr^2}\frac{dw^*}{dr}\right) + \frac{1}{r^2}\left|\frac{dw}{dr}\right|^2\right\},$$

$$I = \frac{1}{2}R_e\left\{-i\omega D(1 + i\eta)\left[\frac{d}{dr}\left(\frac{d^2w}{dr^2} + \frac{1}{r}\frac{dw}{dr}\right)w^* - \left(\frac{d^2w}{dr^2} + \frac{v}{r}\frac{dw}{dr}\right)\frac{dw^*}{dr}\right]\right\}, \tag{A3}$$

where ρ is the surface mass density, D is the flexural rigidity and v is the Poisson's ratio. Substituting equation (A2) into equations (A3) and retaining just the lower powers of $1/kr$, one obtains

$$T = \frac{\rho\omega^2|\alpha|^2}{8\pi|k|}\frac{e^{-\eta k_0 r/2}}{r}, \qquad V = \frac{D|k|^3|\alpha|^2}{8\pi}\frac{e^{-\eta k_0 r/2}}{r},$$

$$I = \frac{\omega D|\alpha|^2}{4\pi|k|}R_e\{(1 + i\eta)(k^3 + k^2k^*)\}\frac{e^{-\eta k_0 r/2}}{r}. \tag{A4}$$

Upon remarking that $k_0^4 = \rho\omega^2/D$ and doing a first order development in η as authorized by (H2), the equality between kinetic energy and potantial energy is established: $T = V$. Moreover, introducing the group velocity of the plate, $c_g = 2\omega/k_0$, yields the power flow I as $I = c_g W$, where the energy density W is defined as the sum of the kinetic energy and the potential energy. Finally, the energy W is found to be proportional to the function G deduced from the power balance. This result highlights that the simplifications (H2) and (H3) are compatible with the power balance.

APPENDIX B: PROOF OF EQUALITY (6)

As the functions G and $\mathbf{H}$ are locally integrable in R^n, they define two distributions also denoted by G and $\mathbf{H}$. Thus, the distribution $\mathbf{div}\,.\,\mathbf{H} + mc_gG$ vanishes in $R^n - \{S\}$, i.e., everywhere except S. By virtue of a well-known theorem, this distribution is a finite linear combination of the derivatives of the Dirac distribution.

Now one can evaluate the order of this distribution. Denote by φ a test function with a compact support K. The value of the distribution D at φ is denoted as $\langle D,\varphi\rangle$ with brackets. Then, the value of the distribution $\mathbf{div}\,.\,\mathbf{H} + mc_gG$ at φ is

$$\langle \mathbf{div}\,.\,\mathbf{H} + mc_gG,\varphi\rangle = -\langle \mathbf{H},\mathbf{grad}\varphi\rangle + mc_g\langle G,\varphi\rangle$$

$$= -\int_K \mathbf{H}\,.\,\mathbf{grad}\varphi \, dM + mc_g\int_K G\varphi \, dM. \tag{B1}$$

So,

$$|\langle \mathbf{div}\,.\,\mathbf{H} + mc_g G,\varphi\rangle| \leq \int_K |\mathbf{H}|\,\mathrm{d}M \times \sup_K |\mathbf{grad}\varphi| + mc_g \int_K |G|\,\mathrm{d}M \times \sup_K |\varphi|. \quad \text{(B2)}$$

Then the order of the distribution $\mathbf{div}\,.\,\mathbf{H} + mc_g G$ is at most equal to one:

$$\mathbf{div}\,.\,\mathbf{H} + mc_g G = a\delta_S + \sum_{i=1}^{n} b_i \frac{\partial \delta_S}{\partial x_i}\,. \quad \text{(B3)}$$

in order to determine the constants a and b_i, one chooses test functions of the form $\varphi(r)$ where $r = SM$. Then

$$\langle \mathbf{div}\,.\,\mathbf{H} + mc_g G,\varphi\rangle = -\gamma_0 \int_0^A H(r) \frac{\mathrm{d}\varphi}{\mathrm{d}r} r^{n-1}\,\mathrm{d}r + mc_g\gamma_0 \int_0^A G(r)\varphi(r) r^{n-1}\,\mathrm{d}r, \quad \text{(B4)}$$

where A is the diameter of the compact K and γ_0 is the solid angle of the space. $\gamma_0 = 2$ for $n = 1$, $\gamma_0 = 2\pi$ for $n = 2$ and $\gamma_0 = 4\pi$ for $n = 3$. Here

$$\begin{aligned}\langle \mathbf{div}\,.\,\mathbf{H} + mc_g G,\varphi\rangle &= -\gamma_0 c_g \int_0^A \mathrm{e}^{-mr} \frac{\mathrm{d}\varphi}{\mathrm{d}r}\,\mathrm{d}r + mc_g\gamma_0 \int_0^A \mathrm{e}^{-mr}\varphi(r)\,\mathrm{d}r \\ &= -\gamma_0 c_g\,[\mathrm{e}^{-mr}\varphi(r)]_0^A = \gamma_0 c_g \varphi(0). \end{aligned} \quad \text{(B5)}$$

The coefficients a and b_i are now identified with the help of $n + 1$ functions φ which are linearly independent one obtains, in more physical notations,

$$\mathbf{div}_M\,.\,\mathbf{H}(S,M) + mc_g G(S,M) = \gamma_0 c_g \delta_S(M). \quad \text{(B6)}$$

This is the local version of the power balance for propagative waves.

APPENDIX C: NOTATION

W	energy density (scalar field)
$\mathbf{I}$	energy flow (vector field)
p_{diss}	power density being dissipated
p_{inj}	injected power density
η	hysteretic damping factor
c_g	group velocity
c_φ	phase velocity
m	acoustic attenuation coefficient
ω	circular frequency
G, $\mathbf{H}$	defined by equation (5): energy density and energy flow associated to a travelling wave
δ_S	delta Dirac function at point S
Ω, $\partial\Omega$	space under consideration and its boundary
n	dimension of the system Ω, $n = 1$, 2 or 3
$\mathbf{u}_{SM}$	unit vector from S to M
$\mathbf{n}_P$	outward unit vector at point P
ρ	actual sources located inside Ω
σ	fictive sources located on $\partial\Omega$

f	directivity function of fictive sources σ
γ_0	solid angle of space Ω
γ	defined by equation (22): a dimensional quantity associated to the directivity f
r	reflection efficiency of the interface
t	transmission efficiency of the interface
k	complex wavenumber
k_0	real wavenumber (undamped system)
R_e	real part of a complex number
*	conjugate of a complex number